Model predictive control for a data centre waste heat-based heat prosumer in Norway

Juan Hou*, Haoran Li, Natasa Nord
Department of Energy and Process Technology, Norwegian University of Science and Technology (NTNU), Trondheim, Norway
* *corresponding author: juan.hou@ntnu.no*

Abstract

Waste heat from a data centre (DC) is a promising heat source because of the evenly distributed load profile and intensive waste heat generation. Many studies have proven the substantial financial benefits for the district heating (DH) operators by integrating DC waste heat with DH systems. However, there is a scarcity of research focusing on the optimal control of the DH system after integrating DC waste heat to further improve the system's economic performance. Therefore, this study aimed to further improve the economic performance of a DH system with DC waste heat by utilizing a model predictive control (MPC) scheme. This MPC scheme employed an economic-related objective function and formulated technical operational constraints. The proposed MPC scheme was tested on a campus DH system in Norway by simulation. Compared to a traditional rule-based control approach, the MPC scheme reduced the monthly energy cost by 1.8% while providing more stable chilled water for the DC cooling system.

Introduction

A data centre (DC) is a location where information technology (IT) equipment is housed. Moreover, a DC usually incorporates environmental control devices to guarantee that the IT equipment operates in a safe environment. These two major energy end-user equipment, i.e. the IT equipment and environmental control devices, results in a DC an energy-intensive facility. A DC can use more than 40 times the energy of a typical office building, and the majority of electricity used in DCs is converted into waste heat [1]. As a result, given the concern on the energy and climate crises, it is critical to investigate techniques for improving the energy efficiency of DCs [2]. The integration of DC waste heat into district heating (DH) systems is an effective way for the sustainability of DC as well as the improvement of the DH system's economic performance, and many researchers have proven it [3-5]. However, there is a scarcity of research focusing on the optimal control of the DH system after integrating DC waste heat to further improve the system economic performance, particularly for a DC waste heat-based heat prosumer with thermal energy storage (TES).

An optimal control technique may fully unlock the system's flexibility and hence further improve the DH system's economic performance. Model predictive control (MPC), which can use an economic-related objective function, is an ideal optimal control technique for achieving the system's maximum feasible economic performance while meeting various technical operational restrictions [6, 7]. In the presence of disturbances and technical operational restrictions, an MPC technique employs a system dynamic model to predict the system's future behaviour and provides an optimal control vector that minimizes an objective function over the prediction horizon.

This study, therefore, aimed to contribute to the optimal control of the DH system after integrating DC waste heat to further improve the system's economic performance by utilizing an MPC scheme. In the MPC scheme, an economic-related objective function based on an economic boundary was defined, a system dynamic model was developed and optimization constraints were formulated based on a real system's measured data. A campus DH system located in central Norway, which is a DC waste heat-based heat prosumer, was chosen as the case system to test the proposed MPC scheme by simulation. Moreover, the campus DH system was monitored by its energy management platform, which provided extensive operational data to aid this study. The DC performance, the total energy use and the energy bill of the system were used to evaluate the proposed MPC scheme. The main contributions of this study are listed as follows. Firstly, this study aimed to explore the optimal control of a DH system after integrating DC waste heat, which is a realistic yet rarely addressed issue. Secondly, the economic boundary was formulated by considering the dynamic pricing schemes of heating and electricity in Nordic countries at the same time, which may contribute to the study of the energy system involving both thermal and electrical networks. Lastly, real measured data from the case system was used to formulate the optimization constraints, which may supplement the recommended values from the standards and support the simulation and optimization to reveal the operation of a real system.

The remainder of this article is organised as follows. Section 2 describes the campus DH system, presents the developed system dynamic model, the developed economic boundary and the formulated MPC scheme. The information on simulation settings and research scenarios is introduced as well in Section 2. The model validation and simulation results are presented in Section 3. Lastly, conclusions are given in Section 4.

Methods

This section describes the campus DH system, as well as the system modelling method and economic boundary

© The Authors, published by EDP Sciences. This is an open access article distributed under the terms of the Creative Commons Attribution License 4.0 (http://creativecommons.org/licenses/by/4.0/).

condition. Finally, the MPC formulation, simulation settings and research scenarios are demonstrated.

Campus district heating system

Figure 1 presents the studied campus DH system, which is located in Trondheim, Norway. The campus DH system is connected to the city DH system via heat exchangers (HEs) in the main substation (MS), allowing the campus DH system to be managed independently. The waste heat from the university DC is captured by heat pump (HP) units and reused for the heating demand of the campus so that the DC waste heat is a distribution heat source (DHS). The connection method between the DC and campus DH system is that the water is extracted from the return pipe of the campus DH system and heated by the high-temperature refrigerant vapour at the HP condenser, and then fed back into the return pipe [8, 9]. Based on the measured data from June 2017 to May 2018, as shown in Figure 2, the total building heating demand was 32.8 GWh. The DC waste heat recovery accounted for about 20% of the total heating supply, and the rest 80% was supplied from the city DH system via the MS. As a result, the DH system on campus is a DC waste heat-based heat prosumer. In addition, buildings with a total building area of around 300 000 m^2 are the heat users in this campus DH system [10].

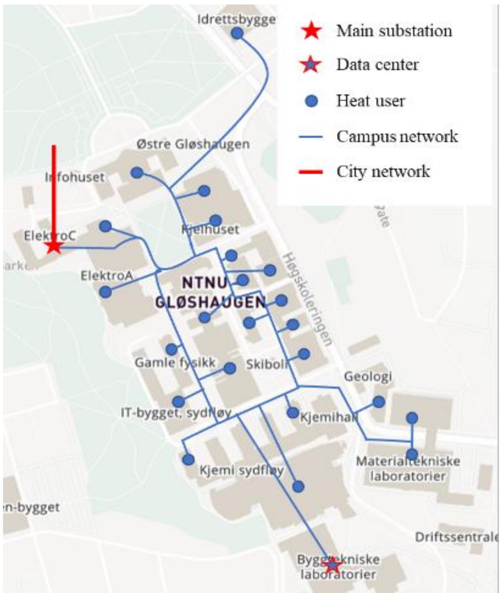

Figure 1. Campus district heating system

Another feature noticed in Figure 2 is that the building heating demand was not equally distributed and hence the peak heat loads were needed from the MS because the DC waste heat supply was almost constant throughout the year. However, the local DH company considers heat users' peak loads and the charging fee based on the peak loads accounted for around 26% of the total heating bill each year. The previous study has shown that using a short-term TES, water tank TES (WTTES), for the case system could solve the high peak load problem while also improving the system's economic performance [11]. Furthermore, research has been conducted to determine the optimal storage size for the introduced WTTES [12]. Therefore, this study was further research based on this previous research and introduced a WTTES with optimal storage size. The introduced WTTES had a storage volume of 900 m^3 and was able to supply heat to the campus DH system for up to 12 hours. In addition, the introduced WTTES was charged by a HE in the MS.

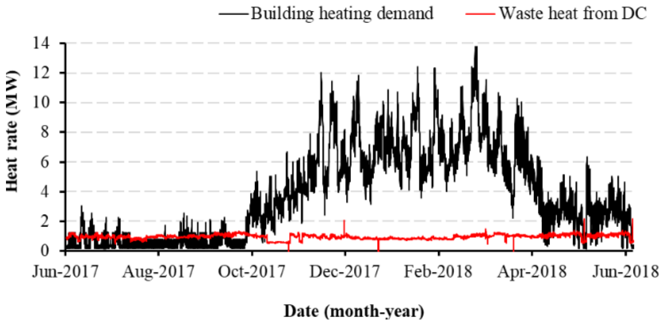

Figure 2. Building heating demand and data centre waste heat recovery

System modelling method

MPC uses a system dynamic model to predict the system's future behaviour and provides an optimal control vector. The Modelica language was used in this study to build the system dynamic model, which was based on the energy and mass flow exchanging connection between the individual component models. The individual components consisted of the MS, DC, buildings, WTTES, circulator pump (CP) and pipeline. The energy and mass flow exchanges between various components, as well as the modelling method for each component of the MS, buildings, WTTES and pipelines, are elaborated in previous research [12]. The modelling methods of the DC's HP and CP are discussed in this section.

Based on research [13], the operational conditions are the key factors that determine an HP's electricity use, aside from the HP's inherent performance characteristics. The operational conditions include the inlet and outlet water temperature as well as the water mass flow rate both at the evaporator and condenser sides of an HP. Moreover, extensive measured data on these operational conditions were available in this study. Therefore, an HP model including these operational conditions was developed, as shown in Equation (1).

$$\hat{E}_{HP} = a \cdot T_{in\_eva} + b \cdot T_{out\_eva} + c \cdot T_{in\_con} + d \cdot T_{out\_con} + e \cdot \dot{m}_{eva} + f \cdot \dot{m}_{con} \quad (1)$$

where $\hat{E}_{HP}$ is the simulated HP compressor power. T_{in_eva} and T_{out_eva} are the inlet and outlet water temperatures at the evaporator side. T_{in_con} and T_{out_con} are the inlet and outlet temperatures at the condenser side. $\dot{m}_{eva}$ and $\dot{m}_{con}$ are the water mass flow rate at the evaporator and condenser sides, respectively. a, b, c, d, e, and f are the parameters needed to be identified. In this study, the Evolutionary engine provided by the Excel Solver was used to identify these parameter values.

To overcome pipeline hydraulic resistance and local pipeline accessory resistance, a CP was employed to circulate warm water for the campus DH network. This study used a variable-speed CP because it can dramatically minimize pumping electricity use [14]. The total pumping power needed to circulate the water in a distribution system can be calculated by Equations (2) and (3).

$$E_{CP} = \frac{\Delta P \cdot \dot{V}}{\eta_{CP}} \tag{2}$$

$$\Delta P = S \cdot \dot{m}^2 \tag{3}$$

where E_{CP} is the CP electricity use. $\dot{V}$ is the water volume flow rate. η_{CP} is the total conversion efficiency of the CP and was 0.7 in this study [15]. ΔP is the total pressure drop of the DH distribution network. $\dot{m}$ is the mass flow rate of water. S is the resistance friction coefficient of the DH distribution network that is related to the characteristics of the pipeline. One assumption was adopted in this study: the water flow rate was regulated by the variable-speed CP, and the pipeline valves had no actions. As a result, the resistance friction coefficient S was a constant value that could be inferred from the DH system's design condition.

Economic boundary condition

The energy bill of the campus DH system includes two parts: 1) heating bill paid for the DH use and 2) electricity bill paid for the electricity use. Heat is provided by the DH company for the HEs in the MS, while electricity is provided by the electricity company for the HP of DC and the CP. As a result, this section defines the economic boundary condition by considering the pricing mechanisms of heating and electricity in Norway at the same time.

A generalized heating price model has been proposed in research [12], and this study used it as well. A generalized electricity price model was proposed in this study based on the investigation of electricity contracts in Norway. When using electricity in Norway, end-users must pay for two components: 1) power price for the electricity purchased from a power supplier, and 2) grid rent to the local grid distribution company for the power's transportation [16, 17].

In terms of the power price paid for a power supplier, a spot-price contract was used in this study. Because it is the most commonly used contract type in Norway based on Statistics Norway [18]. The price of the spot-price contract is calculated by Equations (4), (5) and (6).

$$C_{ele\_pow} = C_{spo} + C_{sur} + C_{mfi} \tag{4}$$

$$C_{spo} = \int_{t_0}^{t_f} PP_{spo}(t) \cdot \dot{E}(t) \cdot dt \tag{5}$$

$$C_{sur} = \int_{t_0}^{t_f} PP_{sur} \cdot \dot{E}(t) \cdot dt \tag{6}$$

where C_{ele_pow} denotes the power price paid by consumers. C_{spo} is the spot price-related fee and C_{sur} is a mark-up fee that must be paid by the customer [19]. C_{mfi} is the monthly fixed fee. Moreover, $PP_{spo}(t)$ represents the spot price at time t and gained from Nord Pool [20]. PP_{sur} is the mark-up fee per energy unit. Finally, $\dot{E}(t)$ is the electricity use at time t.

In terms of the grid rent paid for the grid distribution company, it is determined by the local grid distribution company. The grid rent for a big electricity user includes an energy link fee, a power link fee and an annual fixed fee, as shown by Equations (7), (8) and (9) [21].

$$C_{ele\_gri} = C_{ene} + C_{pow} + C_{afi} \tag{7}$$

$$C_{ene} = \int_{t_0}^{t_f} GP_{ene} \cdot \dot{E}(t) \cdot dt \tag{8}$$

$$C_{pow} = GP_{pow} \cdot \dot{E}_p \tag{9}$$

where C_{ele_gri} denotes the grid rent paid by consumers. C_{ene} and C_{pow} are the energy link fee and the power link fee, respectively. C_{afi} is the annual fixed fee. GP_{ene} is the energy link fee per energy unit and $\dot{E}(t)$ is the electricity use at time t. GP_{pow} is the power extraction price per power unit and $\dot{E}_p$ is the highest hourly power output.

As a result, a generalized electricity price model was suggested in this study, which is determined by Equation (10).

$$C_{ele} = C_{ele\_pow} + C_{ele\_gri} \tag{10}$$

where C_{ele} is the total electricity cost.

Model predictive control formulation

The MPC scheme developed in this study employed an economic-related objective function to further improve the economic performance of the campus DH system. The generalized heating price model and electricity model were used in this objective function. However, the monthly fixed fee in the power price and the annual fixed fee in grid rent were not involved, because they are not determined by the real-time electricity use. Furthermore, the power link fee included in the grid rent of the electricity price model was not taken into account. This is because the optimization problem in MPC only considered the electricity use of the HP and CP, the electricity use by other equipment, lighting, etc. was not considered, while the power link fee is calculated based on the highest hourly total electricity use of the entire energy system. As a result, the MPC controller solves the following optimization problem at each time step:

Minimize:

$$\int_0^H EP(t) \cdot \dot{Q}_{MS}(t) \cdot dt + LP \cdot \dot{Q}_{MS\_p} + \int_0^H (PP_{spo}(t) + PP_{sur} + GP_{ene}) \cdot (\dot{E}_{HP}(t) + \dot{E}_{CP}(t)) \cdot dt \tag{11}$$

subject to:

$$\dot{Q}_{MS}(t) \leq \dot{Q}_{MS\_p} \quad (12)$$

$$F(t, \mathbf{z}(t)) = 0 \quad (13)$$

$$F_0(t_0, \mathbf{z}(t_0)) = 0 \quad (14)$$

$$z_L \leq \mathbf{z}(t) \leq z_U \quad (15)$$

where H is the predictive horizon and was 12 hours in this study. $\dot{Q}_{MS}(t)$ is the heat flow rate from the MS at time t. $\dot{Q}_{MS\_p}$ is the peak heat rate from the MS, and it was a parameter to be optimized in this study. The peak heat rate was determined by the maximum hourly heat use in one month in this study [22]. $EP(t)$ is the energy demand component (EDC) heating price at time t, and LP is the load demand component (LDC) heating price [12]. $\dot{E}_{HP}(t)$ and $\dot{E}_{CP}(t)$ denote the HP electricity use and the CP electricity use at time t, respectively. The system dynamic model and its initial condition are the equality constraints as shown by Equations (13) and (14). Equation (15) defines the inequality constraint, which includes the technical operational constraints. $\mathbf{z} \in \mathbb{R}^{n_z}$ is the set of time-dependent variables and includes the manipulated variables $\mathbf{u} \in \mathbb{R}^{\mathrm{n_u}}$ to be optimized, the differential variables $\mathbf{x} \in \mathbb{R}^{\mathrm{n_x}}$, and the algebraic variables $\mathbf{y} \in \mathbb{R}^{\mathrm{n_y}}$. $z_L \in [-\infty, \infty]^{\mathrm{n_z}}$ and $z_U \in [-\infty, \infty]^{\mathrm{n_z}}$ are the lower and upper limits, respectively.

Finally, the above-formulated optimization problem was solved on the optimization platform JModelica.org [23]. The detailed information on the optimization algorithm used in JModelica .org was elaborated on in the research [24].

Simulation settings and research scenarios

The building heating demand presented in Figure 2 was used as simulation inputs in the study. The energy prices, which included both heating and electricity, were collected from the local DH company [25] and a power supplier [26]. The used LDC in heating price was 39 NOK/kW (The currency rate between NOK and EUR used in this study was 1 EUR=10.0 NOK). The used EDC in heating price ranged from 0.484 to 0.868 NOK/kWh, while the electricity use-related price ranged from 0.485 to 0.870 NOK/kWh. The measured inlet water temperature and water mass flow rate of the evaporator in DC were almost constant values, with the average values of 11°C and 36.5 kg/s, and were directly used as simulation inputs in this study.

An MPC scenario together with an RBC scenario was proposed in the study. The RBC scenario was a reference scenario based on an RBC strategy, as shown in Figure 3 (a). A weather compensation controller (WCC) and a proportional-integral (PI) controller were used to control the supply water temperature and water flow rate of HE2. Another PI controller was utilized to control the compressor power of HP according to the feedback from the outlet water temperature of the evaporator, whose reference value was set as 6.5 °C. Moreover, a pre-defined schedule based on the heating demand characteristics was used to control the charging and discharging processes of WTTES.

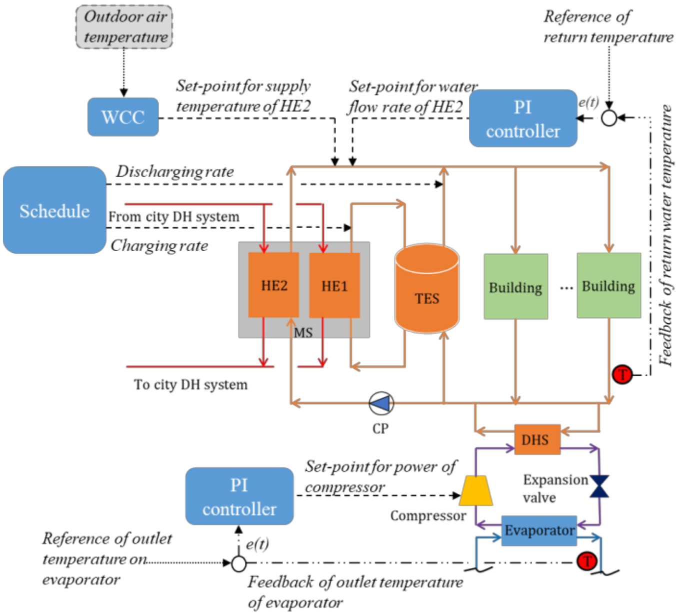

(a) Rule-based control scenario

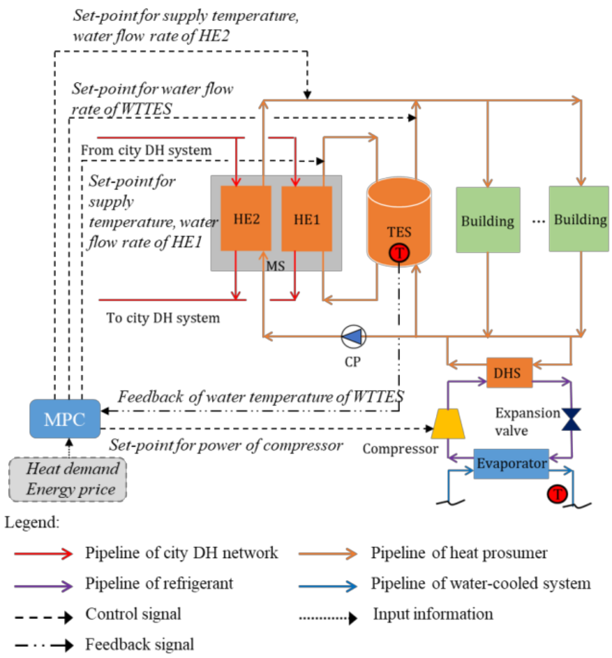

(b) Model predictive control scenario

Figure 3. Research scenarios

The MPC scenario was based on the proposed MPC scheme, as shown in Figure 3 (b). Its manipulated variables included the supply water temperature and mass flow rate of the HEs, the water mass flow rate of the WTTES and the power of the HP compressor. In the real system, these manipulated variables were constrained to their feasible regions, formulating the MPC's technique operational constraints. The bounds of the HP compressor power were obtained by the measured data. The range of the outlet water temperature at the evaporator was set as

https://doi.org/10.1051/e3sconf/202236206007

6.0- 7.0°C based on measured data. The bound settings of other manipulated variables can be found in [12].

Results

This section firstly introduces the model validation and then evaluates the MPC scheme in terms of the DC performance as well as the total energy use and energy bill of the system. In addition, January of 2018 was chosen as a typical month in the heating season of the year 2017-2018 to conduct this simulation-based study.

Model validation

Table 1 shows the values for the identified parameters in the HP model. The HP model was validated by the measured data from the campus energy management platform, as shown in Figure 4. Mean absolute error (MAE), mean absolute percentage error (MAPE) and root mean square error (RMSE) were utilized to evaluate the developed model, as presented in Figure 4 [27, 28]. Moreover, as shown in Figure 4, the simulated compressor hourly power matched the measured data well with the coefficient of determination (R^2) of 0.93.

Table 1. Values of the identified parameters

Parameter	*a*	*b*	*c*	*d*	*e*	*f*
Value	-1.5	10.6	-17.0	24.4	-5.7	-9.3

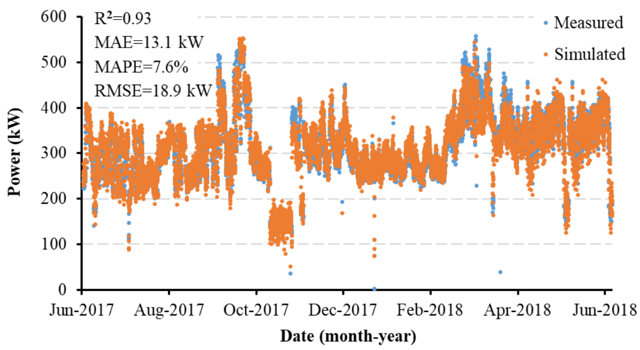

Figure 4. Simulated and measured hourly compressor power of heat pump

Data centre performance

Figure 5 presents the outlet temperature of the evaporator in HP. Compared to the RBC scenario, the MPC scenario had a smaller outlet temperature fluctuating range and preferred lower outlet temperatures with an average value of 6.0. Moreover, one result was obtained as well: the cooling requirement of DC was satisfied in both MPC and RBC scenarios because the evaporator's outlet water temperatures were mostly between 6.0 and 7.0°C, which was the feasible range based on the measured data. Figure 6 presents the coefficient of performance (COP) of HP. Similar to the outlet temperature of the evaporator, the MPC scenario had a lower COP fluctuating range yet higher COP values with an average value of 3.1. These results showed that the MPC scenario was more robust than the RBC scenario, expressed as the lower fluctuation ranges of both the evaporator's outlet temperature and the HP's COP, both of which are critical for the DC cooling system's safe operation.

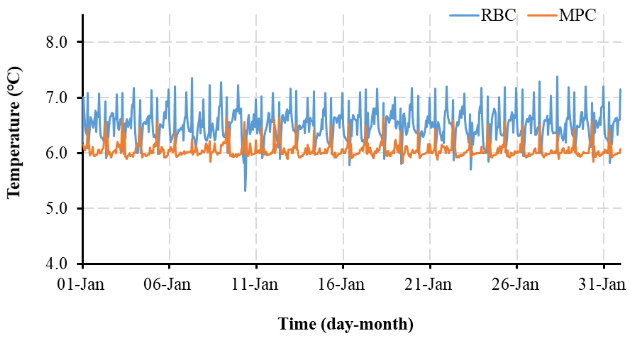

Figure 5. Simulated outlet temperatures of the evaporator

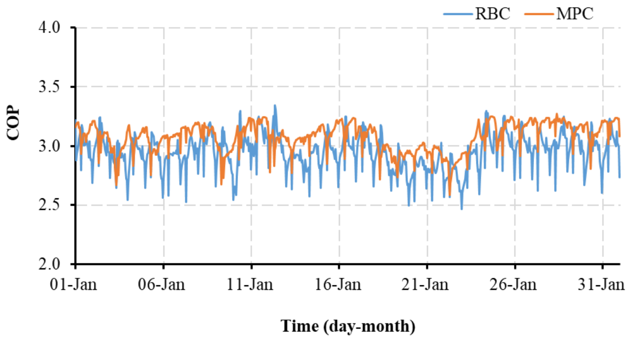

Figure 6. Simulated coefficient of performance of heat pump

Total energy use and energy bill

The total energy use consisted of the heat use from the MS and the electricity use to power the HP of DC and the CP. Figure 7 presents the simulated total energy use in January of 2018 for the two research scenarios. Compared to the RBC scenario, more electricity but less heat were used in the MPC scenario. As shown in Figure 7, the total heat use in the MPC scenario was 5.02 GWh, with a reduction of 2.0% compared to the RBC scenario. In contrast, electricity use was increased by 8.1% in the MPC scenario. The reason can be explained as follows: the MPC scenario preferred to produce more waste heat from the DC by utilizing more electricity because the HP's COPs were usually higher than 1 and fluctuated at 3.1. In addition, during the study period, the electricity prices were only slightly higher than the heating prices. As a result, the MPC scheme depended on obtaining as much heat as possible from the HP to achieve the best possible economic performance.

Figure 8 presents the monthly total energy bill for the two research scenarios. The energy bill included heating and electricity costs. Thereof, the heating cost consisted of the LDC based on the heat user's peak load and the EDC based on the total heat users' heat use. As shown in Figure 8, the MPC scenario saved the total energy bill by 1.8% compared to the RBC scenario. Specifically, the reduced heating costs in the MPC scenario, which were brought by both the reductions of the LDC and the EDC, with a total cost reduction of 2.3%. On the other hand, the MPC scenario increased the electricity cost by 8.2% due to the increased electricity use. However, the electricity cost contributed to less than 10% of the total energy bill and hence the overall economic performance of the MPC scenario was not impaired by the increased electricity cost. In summary, the MPC scheme optimized the trade-off between heat and electricity use so that the possible maximum economic performance of the heat prosumer was achieved in the MPC scenario.

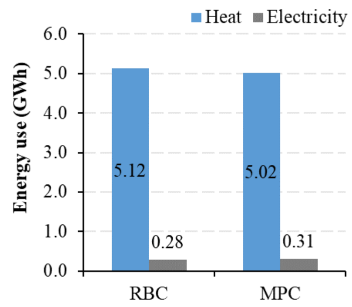

Figure 7. Energy use for the two research scenarios

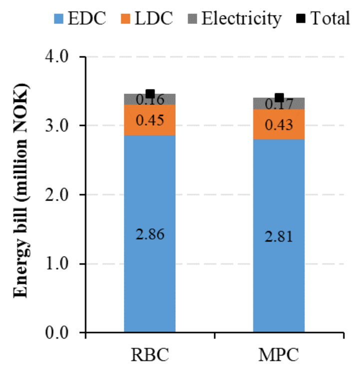

Figure 8. Energy bill for the two research scenarios

Conclusion

This study aimed to further improve the economic performance of a DH system after integrating DC waste heat by utilizing an MPC scheme. The MPC scheme employed an economic-related objective function, formulated the economic boundary condition and the technical operational constraints. The proposed MPC scheme was tested on a campus DH system in Norway by simulation.

Results showed that the MPC scheme was found to be more stable and robust, as seen by smaller fluctuating ranges of both the evaporator outlet temperatures and the COPs of the HP in DC, which are critical for the safe operation of the DC cooling system. To achieve the best possible economic performance, the MPC scheme tended to extract waste heat from the DC as much as possible by utilizing more electricity for the HP but extracting less heat from the MS, resulting in a 1.8% monthly energy cost saving. In summary, the MPC scheme optimized the trade-off between heat and electricity use so that the possible maximum economic performance of the heat prosumer was achieved in the MPC scenario.

Acknowledgement

The authors gratefully acknowledge the support from the Research Council of Norway through the research project Understanding behaviour of district heating systems integrating distributed sources under the FRIPRO/FRINATEK program (project number 262707).

Nomenclature

COP	Coefficient of performance
CP	Circulator pump
DC	Data centre
DH	District heating
DHS	Distributed heat source
EDC	Energy demand component
HE	Heat exchanger
HP	Heat pump
IT	Information technology
LDC	Load demand component
MAE	Mean absolute error
MAPE	Mean absolute percentage error
MPC	Model predictive control
MS	Main substation
PI	Proportional-integral
RBC	Rule-based control
RMSE	Root mean square error
TES	Thermal energy storage
WCC	Weather compensation controller
WTTES	Water tank thermal energy storage

References

[1] Greenberg S, Mills E, Tschudi B, Rumsey P, Myatt B. Best practices for data centers: Lessons learned from benchmarking 22 data centers. Proceedings of the ACEEE Summer Study on Energy Efficiency in Buildings in Asilomar, CA ACEEE, August. 2006;3:76-87.

[2] Huang P, Copertaro B, Zhang X, Shen J, Löfgren I, Rönnelid M, et al. A review of data centers as prosumers in district energy systems: Renewable energy integration and waste heat reuse for district heating. Applied Energy. 2020;258:114109.

[3] Wahlroos M, Pärssinen M, Manner J, Syri S. Utilizing data center waste heat in district heating–Impacts on energy efficiency and prospects for low-temperature district heating networks. Energy. 2017;140:1228-38.

[4] Davies G, Maidment G, Tozer R. Using data centres for combined heating and cooling: An investigation for London. Applied Thermal Engineering. 2016;94:296-304.

[5] He Z, Ding T, Liu Y, Li Z. Analysis of a district heating system using waste heat in a distributed cooling data center. Applied Thermal Engineering. 2018;141:1131-40.

[6] Drgoňa J, Arroyo J, Cupeiro Figueroa I, Blum D, Arendt K, Kim D, et al. All you need to know about model predictive control for buildings. Annual Reviews in Control. 2020;50:190-232.

[7] Killian M, Kozek M. Ten questions concerning model predictive control for energy efficient buildings. Building and Environment. 2016;105:403-12.

[8] Li H, Nord N. Transition to the 4th generation district heating-possibilities, bottlenecks, and challenges. Energy Procedia. 2018;149:483-98.

[9] Nord N, Shakerin M, Tereshchenko T, Verda V, Borchiellini R. Data informed physical models for district heating grids with distributed heat sources to understand thermal and hydraulic aspects. Energy. 2021;222:119965.

[10] Guan J, Nord N, Chen S. Energy planning of university campus building complex: Energy usage and coincidental analysis of individual buildings with a case study. Energy and Buildings. 2016;124:99-111.

[11] Li H, Hou J, Hong T, Ding Y, Nord N. Energy, economic, and environmental analysis of integration of thermal energy storage into district heating systems using waste heat from data centres. Energy. 2021;219:119582.

[12] Li H, Hou J, Tian Z, Hong T, Nord N, Rohde D. Optimize heat prosumers' economic performance under current heating price models by using water tank thermal energy storage. Energy. 2022;239:122103.

[13] Shu H-W, Duanmu L, Zhu Y-X, Li X-L. Critical COP value of heat pump unit for energy-saving in the seawater-source heat pump district heating system and the analysis of its impact factors. Harbin Gongye Daxue Xuebao(Journal of Harbin Institute of Technology). 2010;42(12):1995-8.

[14] Liu X, Zheng ON, Niu F. A simulation-based study on different control strategies for variable speed pump in distributed ground source heat pump systems. ASHRAE Transactions. 2016;122.

[15] Grundfos. Circulator pump, https://product-selection.grundfos.com/no/products/nbg-nbge/nbg/nbg-100-80-160177-97839346?pumpsystemid=1406357823&tab=variant-sizing-results; 2021 [accessed 15 December 2021].

[16] Norwegian Water Resources and Energy Directorate. Energy Regulatory Authority, https://www.nve.no/reguleringsmyndigheten/kunde/nett/nettleie/?ref=mainmenu; 2021 [Accessed 3 November 2021].

[17] Karlsen SS. Investigation of Grid Rent Business Models as Incentive for Demand-Side Management in Buildings-A case study on fully electric operated houses in Norway. Master thesis: Norwegian University of Science and Technology. 2018.

[18] Statistics Norway. Energy and Manufacturing, https://www.ssb.no/en/energi-og-industri/artikler-og-publikasjoner/twofold-increase-in-electricity-price-for-households; 2021 [Accessed 3 November 2021].

[19] Energy Facts Norway. Norway's Energy Supply System, https://energifaktanorge.no/en/utskrift/#toc-2; 2021 [Accessed 3 November 2021].

[20] Nord Pool. https://www.nordpoolgroup.com/; 2021 [Accessed 3 November 2021].

[21] Tensio. Grid Rental, https://ts.tensio.no/kunde/nettleie-priser-og-avtaler; 2021 [Accessed 3 November 2021].

[22] Li H, Hou J, Hong T, Nord N. Distinguish between the economic optimal and lowest distribution temperatures for heat-prosumer-based district heating systems with short-term thermal energy storage. Energy. 2022:123601.

[23] Åkesson J, Årzén K-E, Gäfvert M, Bergdahl T, Tummescheit H. Modeling and optimization with Optimica and JModelica. org—Languages and tools for solving large-scale dynamic optimization problems. Computers & Chemical Engineering. 2010;34(11):1737-49.

[24] Hou J, Li H, Nord N, Huang G. Model predictive control under weather forecast uncertainty for HVAC systems in university buildings. Energy and Buildings. 2021:111793.

[25] Statkraft varme at Tronheim. Products and services, https://www.statkraftvarme.no/globalassets/0/statkraft-varme/produkter-og-tjenester/prisark/jan-2021/trondheim-bedrift-uten-volumledd-bt1.pdf; 2021 [accessed 16 December 2021].

[26] NordlysEnergi. Company, https://www.nordlysenergi.com/bedrift; 2021 [accessed 16 December 2021].

[27] Ahmad T, Chen H, Shair J. Water source heat pump energy demand prognosticate using disparate data-mining based approaches. Energy. 2018;152:788-803.

[28] Wang J, Li G, Chen H, Liu J, Guo Y, Sun S, et al. Energy consumption prediction for water-source heat pump system using pattern recognition-based algorithms. Applied Thermal Engineering. 2018;136:755-66.